ISET Journal of Earthquake Technology, Paper No. 582, Vol. 60, No. 4, December 2023, pp. 113-126

SEISMIC HAZARD MAPPING FOR PEAK GROUND VELOCITY – I: MICROZONATION OF NEW DELHI, INDIA

V.W. Lee
Dept. of Civil Engineering, Univ. of Southern California
Los Angeles, CA, 90089, USA, E mail id: *vlee@usc.edu*

M.D. Trifunac
Dept. of Civil Engineering, Univ. of Southern California
Los Angeles, CA, 90089, USA, E mail id: *misha.trifunac@gmail.com*

I.D. Gupta (Corresponding author)
Independent Scholar, Row House 4, Suncity
Pune 411051, India. E mail id: *idgrh4@gmail.com*

ABSTRACT

We present the probabilistic seismic microzonation maps for V_{max}, peak velocity of strong earthquake ground motion, for New Delhi. We show how these maps can be used to evaluate the strains near ground surface during strong ground motion, the areas where buildings can be damaged during future strong ground motion. We also show that how V_{max} together with probabilistic estimates of relative displacement spectra can be used to derive estimates of pseudo static forces in ground level columns of long structures.

KEYWORDS: Probabilistic Maps of V_{max}; Peak Ground Strains; Differential Ground Motion; Pseudo Static Forces in Ground Floor Columns

INTRODUCTION

Traditional ground motion scaling in studying the response of engineering structures has been in terms of standard spectral shapes anchored to peak ground acceleration. This simplified approach neglects the frequency dependence of the spectral amplitudes of ground motion on earthquake magnitude, site conditions and probability of exceedance (Trifunac 1992, 2013, 2016). Furthermore, many required engineering scaling parameters and functions are not well correlated with the peak ground acceleration. For example, estimation of maximum pseudo static forces in structures caused by differential ground motion (Trifunac and Toodorovska 1997; Trifunac and Gičev 2006), estimation of peak strains near ground surface (Trifunac and Lee 1996; Todorovska and Trifunac 1996a,b), or simple criteria for the threshold levels of strong ground motion amplitudes leading to damage of structures (Duvall and Fogelson 1962) are all directly related to and suitably scaled by peak strong motion ground velocity V_{max} and not by the peak ground acceleration.

In this paper we present seismic microzonation maps of V_{max} for the metropolitan area of New Delhi, and show several examples on how those can be used for scaling in engineering design applications. We show how hazard mapping can be performed for contributions from three seismic source areas, which are associated with three different scaling and attenuation equations. The maps we present complement and should be used together with the seismic microzonation maps for Uniform Hazard Spectra of strong ground motion in New Delhi (Gupta et al. 2022b).

SITE PROPERTIES, STRONG MOTION DATA AND METHODS OF ANALYSES

Computation of seismic hazard maps requires preparation of a comprehensive description of seismic activity surrounding the site (Gupta et al. 2022a), availability of scaling (attenuation) equations (Appendix A; Gupta and Trifunac 2023), a method for probabilistic integration of all earthquake contributions, from all sources affecting the site during a period of Y years of exposure (Appendix B), and spatial distribution of local geological site parameters for the area where hazard mapping is to be performed. As the local soil site parameters typically vary rapidly from point to point, their detailed spatial maps are impractical to make, and hence are best determined for each site via site specific investigations during site preparation for construction. Therefore, in this paper, we will present maps which incorporate geological site conditions, but are presented separately for three soil site parameters $s_L = 0$, 1 and 2 (“rock” soil, “stiff” soil and “deep” soil respectively).

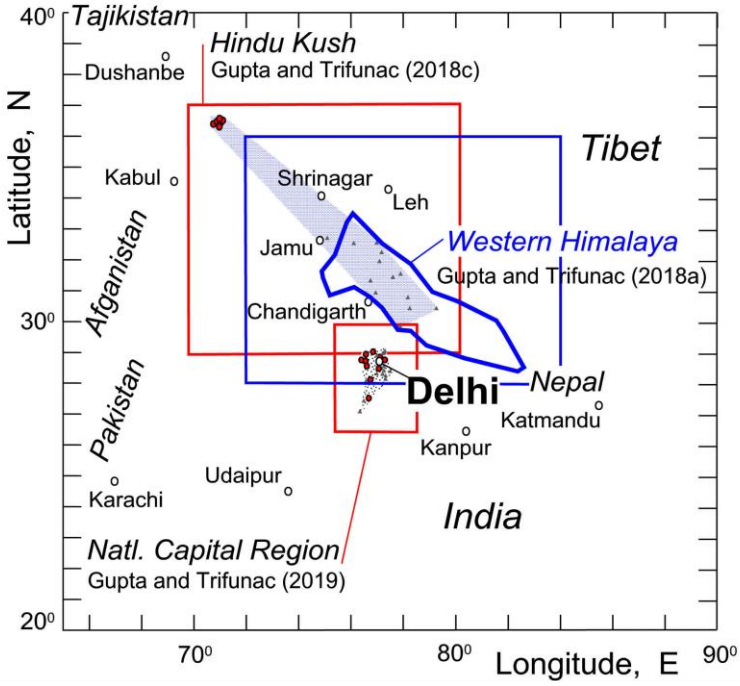

Fig. 1 Earthquake source areas along the Himalayan orogenic belt: Northwestern Himalaya (NWH), Hindu Kush Subduction (HKS), and the National Capital Region (NCR) (Gupta and Trifunac, 2017, 2018 a, b, c, 2019), which contribute to the shaking hazard in New Delhi

Seismic activities in HKS, NWH and NCR, which contribute to seismic hazard in New Delhi, have been described in some detail in our previous work (Gupta et al. 2022a), and for brevity of this presentation will not be repeated here. In this paper we will use the same spatial distribution of earthquake sources as described in Gupta et al. (2022a). For Hindu Kush earthquakes, which occur about 1000 km away from Delhi, we will use the equivalent point source (Gupta and Trifunac (2018c). For earthquake in Northwest Himalaya (NWH) (Gupta and Trifunac 2018a) and in the National Capital Region (NCR) (Gupta and Trifunac 2019), we will use the maps, which describe the spatial distribution of seismic activity as given in Gupta et al. (2022a), in their Figures 5, 6 and 8. The earthquakes in Northeast India (Gupta and Trifunac 2017) and in the Burma subduction zone (Gupta and Trifunac 2018b) are too far to contribute significantly to the hazard in New Delhi area.

For microzonation mapping of $V_{\max}$ in New Delhi it is necessary to consider three different attenuation equations for $V_{\max}$. One describing attenuation from local earthquakes in NCR, one from large distant earthquake in HKS and one from the earthquakes in NWH, north of Delhi (Figure 1). For completeness of this presentation Appendix A describes briefly those three attenuation equations, extracted and abbreviated from Gupta and Trifunac (2023).

A geological map of the Delhi metropolitan area is available at the official website of the Geological Survey of India (https://bhukosh.gsi.gov.in/Bhukosh/Public). Geological formations in the area belong to the Pre-Cambrian and the Quaternary periods (Gupta et al. 2022a). Figure 2 shows the distribution of geological site parameters s in rectangular area 76.7° to 77.5° east and 28.2° to 29.0° north, within which the microzonation hazard maps are shown in this paper. The width and height of this rectangle are divided into cells each with 15’’x15’’ or 0.463 km NS and 0.407 km EW, with area of 0.188 km². We assigned geological site parameters to each cell following the site classification adopted in Trifunac and Brady (1975) and described in Trifunac (2016).

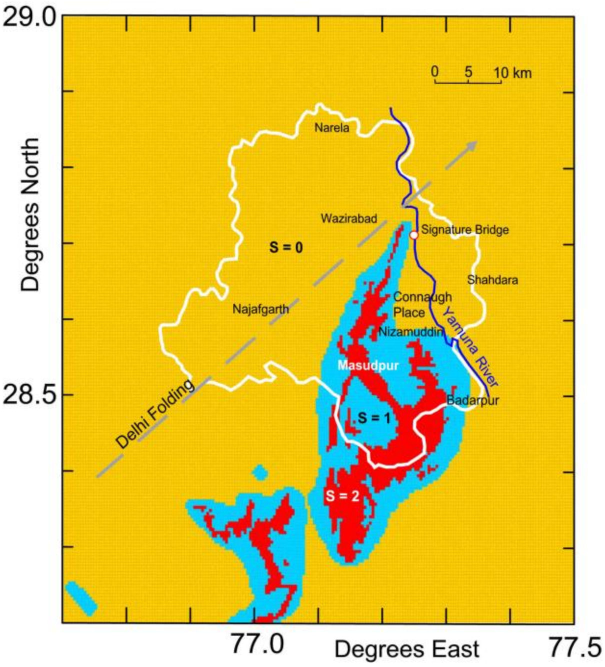

Fig. 2 Geological site parameters $s = 0$ (sediments), $s = 1$ (intermediate sites) and $s = 2$ (basement rock sites) following Trifunac and Brady (1975) geological site classification for use in empirical scaling of strong motion amplitudes. Irregular white line outlines the National Capital Territory (NCT) of the Metropolitan New Delhi. The site of the Signature Bridge on Yamuna River is also shown

RESULTS

Figures 3a, 3b and 3c show the microzonation maps of $V_{\max}$ for Delhi Metropolitan area within the rectangular area shown in Figure 2. Contours of the $V_{\max}$ are shown on logarithmic scale, for exposure during Y=50 years, respectively at soil sites $s_L = 0$ (rock soil), $s_L = 1$ (stiff soil), and $s_L = 2$ (soft soil) and for probabilities of at least one exceedance equal to 10%.

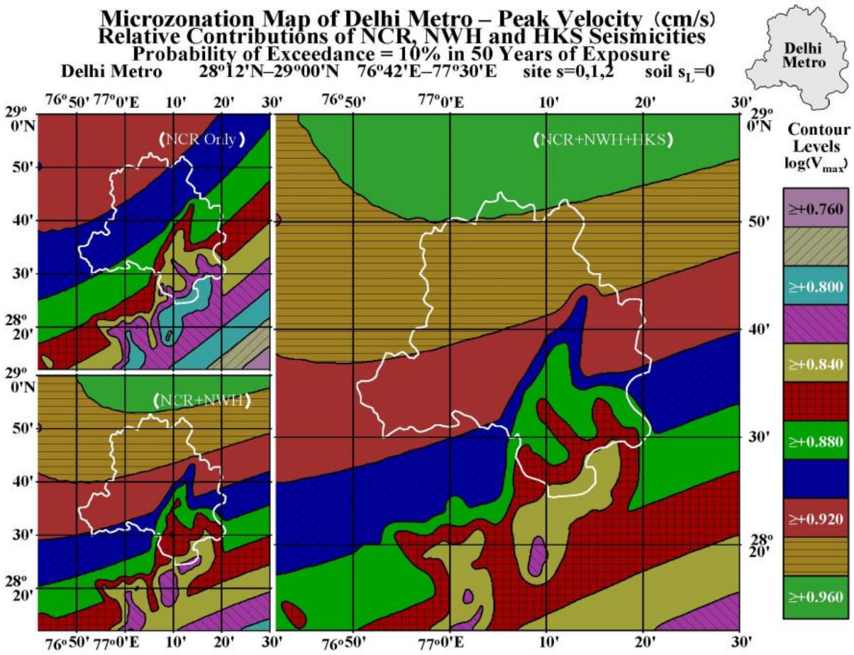

Fig. 3a Seismic microzonation map of Delhi: $\log_{10}(V_{\max})$ contours in cm/s, for Y = 50 yrs exposure and probability of exceedance P = 10%, for sites on rock soil ($s_L = 0$)

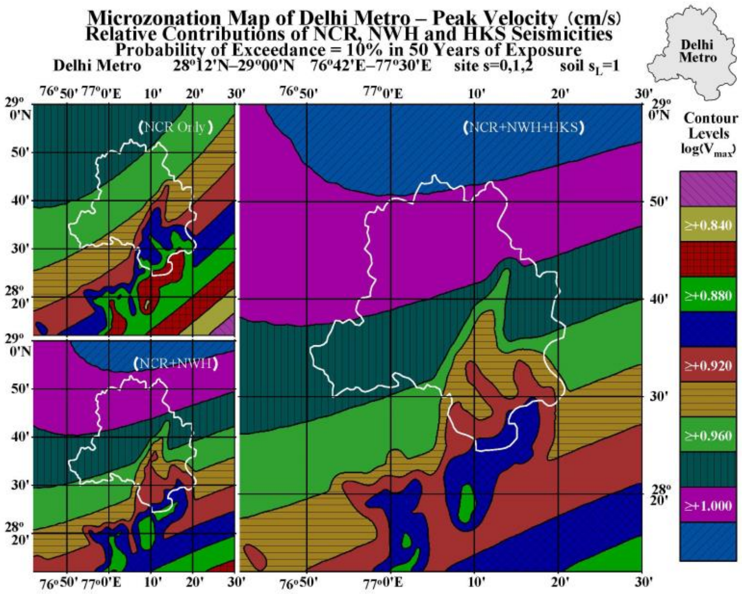

Fig. 3b Seismic microzonation map of Delhi: $\log_{10}(V_{\max})$ contours in cm/s, for Y = 50 yrs exposure and probability of exceedance P = 10%, for sites on stiff soil (s_L = 1)

In Figures 3a, 3b, 3c there are three contour plots: the smaller contour plot on top left shows results due to seismicity only from seismic zone NCR, while the bottom left shows the results due only from seismicities in zones: NCR and NWH. The large contour graph on the right shows the results due to contributions from all three seismic zones: NCR, NWH and HKS. It is seen that the largest contribution is from NCR and the smallest from the distant HKS zone.

It is seen from Figures 3a, b, c that for all three soil sites $s_L = 0$ (rock site), $s_L = 1$ (stiff site) and $s_L = 2$ (deep soil site), the geological site parameter, *s*, has the prominent influence on the contours of $V_{\max}$. The largest amplitudes of $V_{\max}$ occur in the areas covered by sediments (s = 0) (see Figure 2). The smallest amplitudes occur at sites on basement rock (s = 2). This dominant role of geological site condition on contours of $V_{\max}$ is also seen in other microzonation maps, which show spectral amplitudes of strong ground motion (e.g. Gupta et al. 2022b).

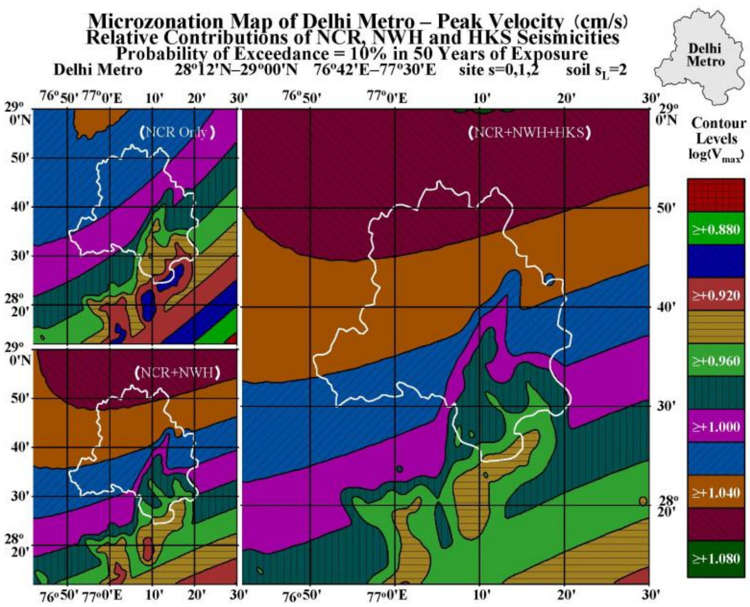

Fig. 3c Seismic microzonation map of Delhi: $\log_{10}(V_{\max})$ contours in cm/s, for Y = 50 yrs exposure and probability of exceedance P = 10%, for sites on deep soil (s_L = 2)

Figure 3d shows the ratios of $V_{\max}$ with contributions from one, two or all three seismic zones: NCR, NWH and HKS, for exposure during Y=50 years, at soil site s_L =1 (stiff soil), and for probabilities of at least one exceedance equal to 10%. Only the case for stiff soil (s_L =1) is included here as the other two cases, rock soil (s_L =0) and soft soil (s_L =2) are similar. In Figure 3d**,** there are two contour graphs: with the one on the left showing the $V_{\max}$ ratio for $V_{\max}\left(NCR+NWH\right)/\,V_{\max}\left(NCR\ only\right)$ while the one on the right is for $V_{\max}\left(NCR+NWH+NKS\right)/\,V_{\max}\left(NCR\ only\right)$, showing the contributions from all thee seismic zones: NCR, NWH and HKS. It is seen that the local seismicity from the National Capital region (NCR) contributes most, while the seismic activities in northwestern Himalaya (NWH) and in the distant Hindu Kush subduction zone (HKS) affect the micronation map only slightly.

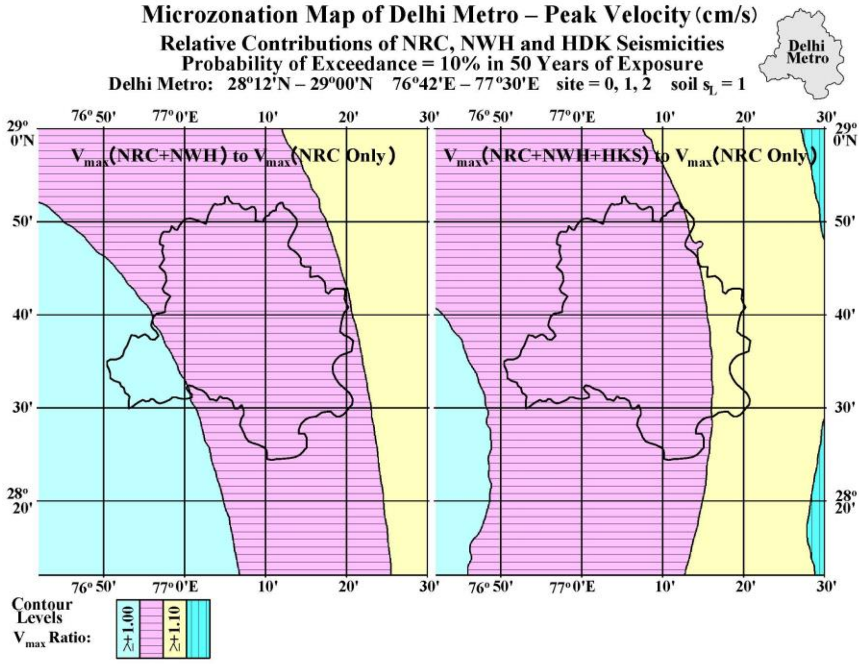

Fig. 3d Seismic microzonation maps of Delhi: relative level of contributions to $V_{\max}$ from NCR, NWH and HKS, for Y = 50 yrs exposure and probability of exceedance P = 10%, for sites on stiff soil (s_L =1)

EAMPLES OF PRACRTICAL USES OF $V_{\max}$

1. Maximum Strain in the Soil Near Ground Surface

The strain in the soil accompanying seismic wave propagation can be approximated by $V_{\max}/\beta$, where β is the shear wave velocity in the soil near ground surface (Todorovska and Trifunac 1996a,b). We illustrate this by assuming uniform β = 100 m/s (10,000cm/s) in the soil everywhere, by simply dividing the results in Figure 3b by a factor equal to 10^4 ($V_{\max}$ in units of cm/s). For values of β which are different from 100 m/s simple multiplication by a constant describing the ratio of desired β relative to 100 m/s will produce the estimates of strain at any point in the area.

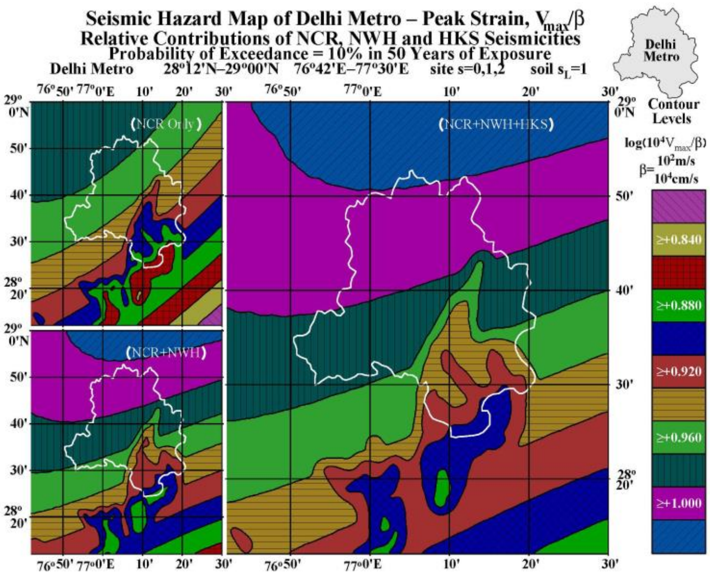

Fig. 4 Contours of peak strain $V_{\max}/\beta$ for Y = 50 yrs exposure and probability of at least one exceedance P = 10%, for sites on stiff soil (s_L = 1)

As expected, β varies rapidly over short distances, so that for a particular engineering project it is necessary to measure β by local site investigations. For a subway line, for example, measurements of β at suitably selected points along the line and then dividing $V_{\max}$ by the measured values of β will produce the desired design values for probabilistically estimated surface strains.

Figure 4 shows the microzonation map of strain, $10^4 V_{\max}/\beta$ for Delhi Metropolitan area. It shows contours of the strain amplitudes, on logarithmic scale, for exposure during Y=50 years, at soil site s_L =1 (stiff soil), and for probability of at least one exceedance equal to 10%. Under those conditions the largest strains occur in the northern portion of the metropolitan area and are equal to 10^{-3}.

2. Empirical Criteria for Damage in Buildings Caused by Ground Shaking

One of the simplest criteria for forecasting the expected damage to buildings due to strong ground motion has been described by Duvall and Fogelson (1962) and is reviewed in detail by Gupta et al. (2003) in terms of peak ground velocity $V_{\max}$.

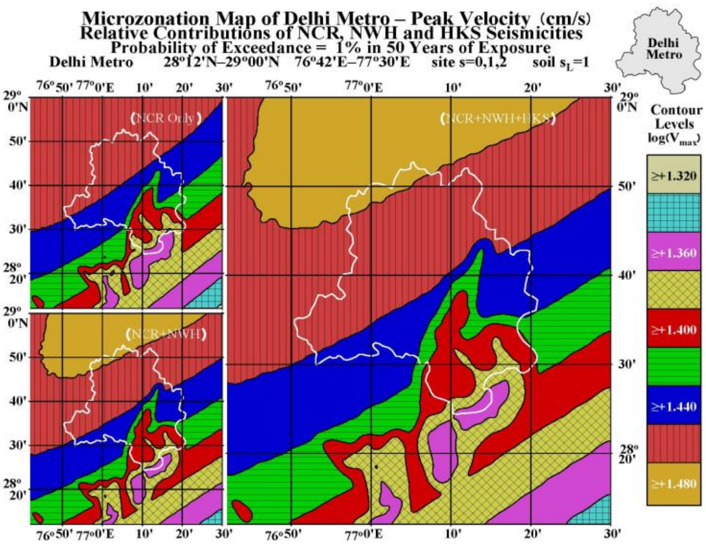

Fig. 5 Seismic microzonation map of Delhi: $\log_{10}(V_{\max})$ contours in cm/s, for Y = 50 yrs exposure and probability of exceedance P = 1%, for sites on stiff soil (s_L = 1)

According to Duvall and Fogelson the damage to building begins when V_{max} approaches and then exceeds 5 cm/s. This can be used as a rough predictor for outlining the areas where damage may occur during future earthquakes.

Referring to Figure 5, for example, it is seen that for probability of at least one exceedance equal to 1%, during exposure of Y=50 yrs, and sites on stiff soil (s_L = 1), the areas in Delhi, can experience strong motion velocities which range from 23 cm/s in the south to 30 cm/s in the north. From lower left segment in Figure 5 it is seen that the contributions to those levels of shaking come mainly from NCR and NWH, with HKS earthquakes contributing negligible amount.

Figure 6 shows that in the northern Delhi (north of Wazirabad), during exposure of Y = 50 years the peak ground velocity can exceed the damage threshold level of 5 cm/s for probabilities of at least one exceedance less than 35%.

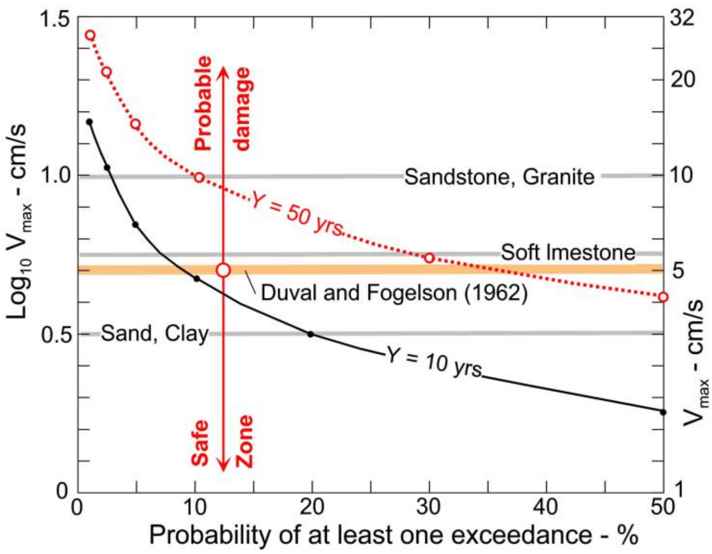

Fig. 6 Peak ground velocity in northern Delhi (north of Wazirabad, see Figure 2) on sediments (s = 0) and stiff soil (s_L = 1), versus probability of at least one exceedance during exposure of Y = 10 and 50 years. Duval and Fogelson (1962) frequency- and site -independent threshold for initiation of damage at 5 cm/s and the refined Langefors and Kihlström (1978) threshold levels which consider the role of sites properties (sand, clay, soft limestone, sandstone, granite) are also shown

The characteristics of ground motion, which contribute to the damage, are of course more complex than just the amplitude of V_{max}. Frequency of motion, duration of motion, the type of dominant waves and distance to the source of waves all contribute, but are averaged out by one-parameter approximation in the Duval and Fogelson (1962) approach. The threshold of damage also depends on the geological and soil site properties. How it varies from soft sites (e.g. sand and clay; 3 cm/s) to hard sites (e.g. sandstone, granite; 10 cm/s) is described in Langefors and Kihlström (1978) and is illustrated in Figure 6.

3. Differential Ground Motion

When one or more dimensions of the plan of a structure become large (buildings with large plan dimensions, bridges, tunnels, pipelines etc), the classical assumption that a motion of the point where structure is attached to the ground can be used to describe the response ceases to be valid. In those cases, it must be assumed that the ground motion varies at the contact points with structure and the response analysis must consider those spatial variations of ground motion. This is illustrated in Figure 7a for the case of in-plane excitation (e.g. Rayleigh waves) where it is seen that the individual columns connecting the structure with ground experience different relative displacements and hence their pseudo static deformations must be included in the analysis of columns, in addition to the simultaneous action by the inertial forces. Figure 7b shows schematically the out of plane response of the columns of a long structure excited by the SH or Love waves, which propagate along the long dimension of the structure.

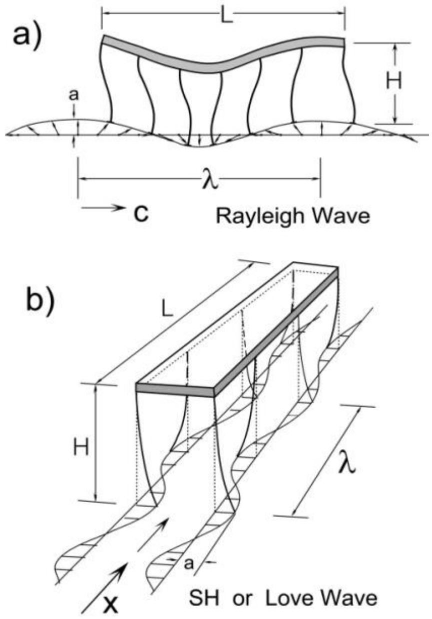

Fig. 7(a) In plane response of a long structure to excitation by Rayleigh waves and (b) out of plane response for SH and Love wave excitation

The in-plane motion in Figure 7a was studied by Trifunac and Todorovska (1997), while the out of plane problem in Figure 7b was analyzed by Trifunac and Gičev (2006). In both cases the spectral displacement of columns, SDC in cm, for analysis of the forces in columns can be approximated by

$$SDC(T) \approx \left\{ SD^2 + f\left(V_{\max}\tau\right)^2 \right\}^{1/2}$$

where $SDC(T)$ is the relative displacement spectrum in cm/s to be used in the design of columns. SD is the classical relative displacement spectrum of a single degree of freedom system in cm at oscillator period T (Trifunac 2012), $V_{\max}$ is the peak ground velocity and τ is approximately the travel time of the waves in the ground required for the waves to travel from one end of the structure to another. The factor f = 1 for in plane deformation of columns (Trifunac and Todorovska 1997) while f = 2 for the out of plane response of columns (Trifunac and Gičev 2006).

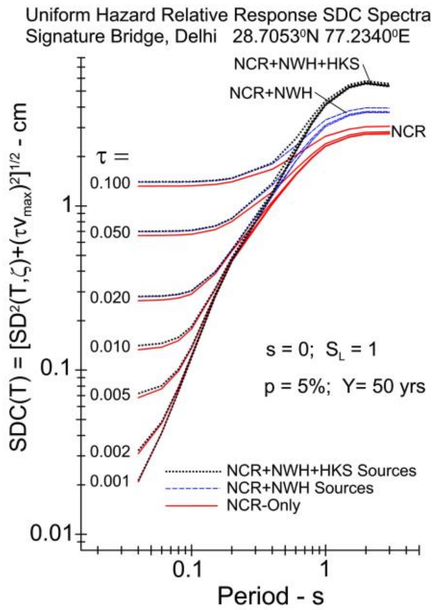

Fig. 8 Uniform hazard SDC spectra at the site of Signature Bridge on Yamuna River, for in-plane response (f = 1)

We illustrate $SDC(T)$ for the site of Signature Bridge on Yamuna River in New Delhi (https://en.wikipedia.org/wiki/Signature_Bridge), a new bridge, constructed during five years, from 2010 to 2016 (Appendix C).

It is seen from Figure 8 that the governing contribution to the $SDC(T)$ spectra is from NCR for short periods $T < 0.5$ s. The increase in $SDC(T)$ amplitudes due to seismicity in NWH and HKST is small. HKS and NWH contribute significantly for periods longer than T = 1 sec.

The assumption in the above equation for $SDC(T)$ is that the strain in the soil between adjacent columns can be approximated by a constant. The main span of the Signature Bridge is 251m, which is too long to approximate the strain between the bridge supports by a constant value. For dynamic analysis of this segment of the bridge it is necessary to employ methods for synthetic generation of strong ground motion to estimate differential motion between the supports. On the other hand, for side spans of Signature Bridge the column spacing is only 36 m (see Figure C1b in Appendix C) and there the above approximation should be valid to estimate $SDC(T)$. For in-plane response of the bridge to Rayleigh waves (f = 1) with phase velocity in the range near 500 m/s, for example, $\tau \sim 0.07$, and from Figure 8 it is seen that the relative displacement of the columns supporting the access to the main span of Signature Bridge can be on the order of 1 cm. For out of plane response, f = 2, and the above estimates are doubled.

CONCLUSIONS

We have presented the microzonation maps for peak strong motion velocity of earthquake ground motion, $V_{\max}$, for New Delhi in India. We showed how hazard mapping can be performed for contributions from three seismic source areas, which are associated with three different scaling and frequency-dependent ground motion attenuation relations. We have illustrated the practical application of the results in (a) estimation of spatial variations of strain, accompanying earthquake ground motion, near ground surface, (b) mapping the areas where future earthquakes can lead to damage of buildings, and (c) analysis of the role of differential strong ground motion for pseudo static action on the ground columns of long structures.

1. APPENDIX A – Empirical Attenuation Equations

The formulation of the empirical scaling and attenuation equations of peak velocity, V_{max}, will follow that of pseudo relative velocity spectra, $PSV(T)$, as given in Gupta et al (2022b). As for *PSV(T)*, it will be for NCR, NWH, and NKS regions contributing the earthquake events to the Delhi metropolitan area. The frequency-dependent attenuation function in the general scaling relations for *PSV(T)* is now replaced by the attenuation function $A_0(T)$ scaled separately for the NCR, NWH and HKS earthquakes. The regression equation for the V_{max} amplitudes then takes the form

$$\begin{aligned}\log_{10} V_{\max} &= M + A_0 \log_{10} \Delta + C_1 + C_2 M + C_3 M^2 + \\ &\quad + C_4 v + C_5 s + C_6^0 S_L^0 + C_6^1 S_L^1 + C_6^2 S_L^2\end{aligned} \qquad (A1)$$

Here, $V_{\max}$ in cm/sec represents the expected value of the peak velocity, M denotes the earthquake magnitude, v denotes the direction of motion ($v=0$ for horizontal and 1 for vertical), s denotes the site geology parameter (s = 0 for sediments, 1 for intermediate sites, and 2 for basement rock sites), and S_L^0, S_L^1, and S_L^2 are variables taking on the value of 1 for the soil site parameters s_L = 0, 1, and 2 and are zero otherwise. The coefficients C_1, C_2, C_3, C_4, C_5, C_6^0, C_6^1 and C_6^2 are obtained by regression. The values of these scaling coefficients are presented in Gupta and Trifunac (2023) for the National Capital Region, the Western Himalaya and the Hindu Kush earthquakes.

The coefficient $\hat{C}_4$ in Eq. (1) is multiplied by v, which is 0 for the horizontal components and 1 for vertical components of ground motion. Since all results in this paper are presented only for horizontal motions, one simply adds $\hat{C}_4$ to $\log_{10} V_{\max}$ or for the linear amplitude scale, multiplies $V_{\max}$ by $10^{\hat{C}_4}$ to convert to the vertical motion results. In the present analysis, from Table 1 below, add $\hat{C}_4 = -0.28$ to get vertical V_{max} in logarithmic scale. On linear scale, this amounts to vertical V_{max} being $10^{-0.28} = 0.525$ times the horizontal V_{max}.

The attenuation term, $A_0 \log_{10} \Delta$ (Gupta and Trifunac, 2023), is defined in terms of the representative distance Δ from the earthquake source to the site under consideration as proposed by Gusev (1983):

$$\Delta = S\left(\ln \frac{R^2 + H^2 + S^2}{R^2 + H^2 + S_0^2} \right)^{-\frac{1}{2}} \tag{A2}$$

where R is the epicentral distance, H is the focal depth, S is the (magnitude-dependent) source size, and S_0 is the correlation radius of the source function:

$$S = \begin{cases} 0.2 \quad \text{for } M \le 3.0 \\ 0.2 + (S_{6.5} - 0.2)(M-3)/3.5 \quad \text{for } 3.0 < M \le 6.0 \\ 13.96 \quad \text{for } M > 6.0 \end{cases} \tag{A3}$$

Here, $S_{6.5}$ is the fault rupture length for M = 6.5, which is obtained from the following relationship as 16.25 km:

$$\begin{aligned} L(M) &= 0.0032 \times 10^{0.57M} \\ W(M) &= 0.0278 \times 10^{0.41M} \text{ for } M \ge 6 \\ W(m) &= L(m) \text{ for } M < 6. \end{aligned} \tag{A4}$$

$$S_0 = \min\left(\frac{\beta T}{2}, \frac{S}{2} \right) \tag{A5}$$

where β is the shear wave velocity at the earthquake source, taken equal to 3.5 km/s in the present study. Value of T is taken as 1.0 s for peak velocity amplitudes. The correlation radius S_0 for the peak displacement is given by (Gusev 1983) as

$$S_0 = \min\left(S_f, S\right)/2 \tag{A6}$$

with (Gupta and Trifunac, 2023):

$$S_f = \begin{cases} L(M) & \text{for } M < 3.5 \\ \dfrac{L(M)}{2.2} + \dfrac{W(M)}{6.0} & \text{for } 3.5 \le M \le 7.0 \\ \dfrac{L(M_{max})}{2.2} + \dfrac{W(M_{max})}{6.0} & \text{for } M > M_{max} = 7.0 \end{cases} \tag{A7}$$

Further, very close to the source (say, hypocentral distance less than 5 km) and for M<4.5, the representative distance Δ for the case of peak displacement is approximated by

$$\Delta = S\left(\ln\left(\frac{S}{S_0} \right)^2 \right)^{-1/2} \tag{A8}$$

with the source size defined such that it is equal to the value of S for M = 4.5 with the magnitude dependence as per the empirical relationship

$$S = 0.0193(5.5 - M) \times 10^{0.57M} \tag{A9}$$

Table 1 from Gupta and Trifunac (2023), gives the regression coefficients (except C_1), C_2, C_3, C_4, C_5, C_6^0, C_6^1 and C_6^2, which will be assumed to be applicable to all the regions in the present analysis.

Table 1: (from Table 2 of Gupta and Trifunac, 2023). Regression Coefficients Defining the Dependences on the Earthquake Magnitude, Component of Motion, Site Geological Condition and Site Soil Condition for all Regions

Parameter	v_{max} (cm/s)
C_2	-0.10143
C_3	-0.02590
C_4	-0.27978
C_5	-0.02243
C_6^0	-0.00798
C_6^1	0.05127
C_6^2	0.09961

and, from the subsequent tables given in Gupta and Trifunac, 2023:

$$A_0 \log\Delta + C_1 = \begin{cases} -1.03589\log\Delta - 2.37314 & \text{for NWH Earthquakes (their Table 4)} \\ -1.59460\log\Delta - 1.43426 & \text{for NCR Earthquakes (their Table 5)} \\ -0.83173\log\Delta - 2.76590 & \text{for HKS Earthquakes (their Table 7)} \end{cases} \quad \text{(A10)}$$

2. APPENDIX B – Probabilistic Hazard Computation

The probability $p[V_{\max}]$ that peak velocity amplitude $V_{\max}$ will be exceeded at least once in Y years is given by (Gupta, 2007):

$$p[V_{\max}] = 1 - e^{-N_E[V_{\max}]} \quad \text{(B1)}$$

where $N_E[V_{\max}]$ = the expected number of times that $V_{\max}$ will be exceeded at the site in Y years. The recurrence time, denoted by $T[V_{\max}]$, of given amplitude $V_{\max}$ is then

$$T[V_{\max}] = N_E[V_{\max}]^{-1} \quad \text{(B2)}$$

for a time unit of Y years. For the examples illustrated in this work, Y will be taken to be 10 and 50 years, but in the specific applications it should be selected by the user. The expected number of exceedances, $N_E[V_{\max}]$, is (taking the logarithm of Eq. (B1))

$$N_E[V_{\max}] = -\ln\left(1 - p[V_{\max}]\right) \quad \text{(B3)}$$

The computer program used for calculations, EQRISKS, is the most recent version of the Anderson and Trifunac program, which has been continuously upgraded and generalized during the past three decades (Gupta et al. 2022b; Lee and Trifunac, 1985, 1987; Todorovska and Trifunac, 1998; Todorovska et al., 2007). In the examples presented in this paper, all sources in the region contributing to the hazard will be represented by a Poissonian sequence in time.

Note that EQRISK can take a combination of events, some of which are Poissonian in time and some that will occur with certainty, and can include also the time-dependent occurrence rates (when seismic sources include identified characteristic events, for example). In the examples shown in this paper, we will not consider such cases, but note that this is a possible alternative for more advanced site-specific modeling. This also means that if an earthquake prediction is made, one can use the probabilistic hazard calculations and existing microzonation maps to evaluate the impact of such a prediction, and where and by how much such a prediction may change the results based on the Poissonian process only.

3. APPENIX C – Signature Bridge

Signature bridge, over Yamuna river at Tarun Goyat in New Delhi is a cantilever spar cable stayed bridge with main span 675 m long (Figures C1a and C1b) at 28.7053°N, 77.2340°E. The bridge is 165 m high and 35.2 m wide. The pylon is made of reinforced concrete, while the bridge deck is made of steel.

Fig. C1a View of Signature Bridge over Yamuna River (looking towards north)

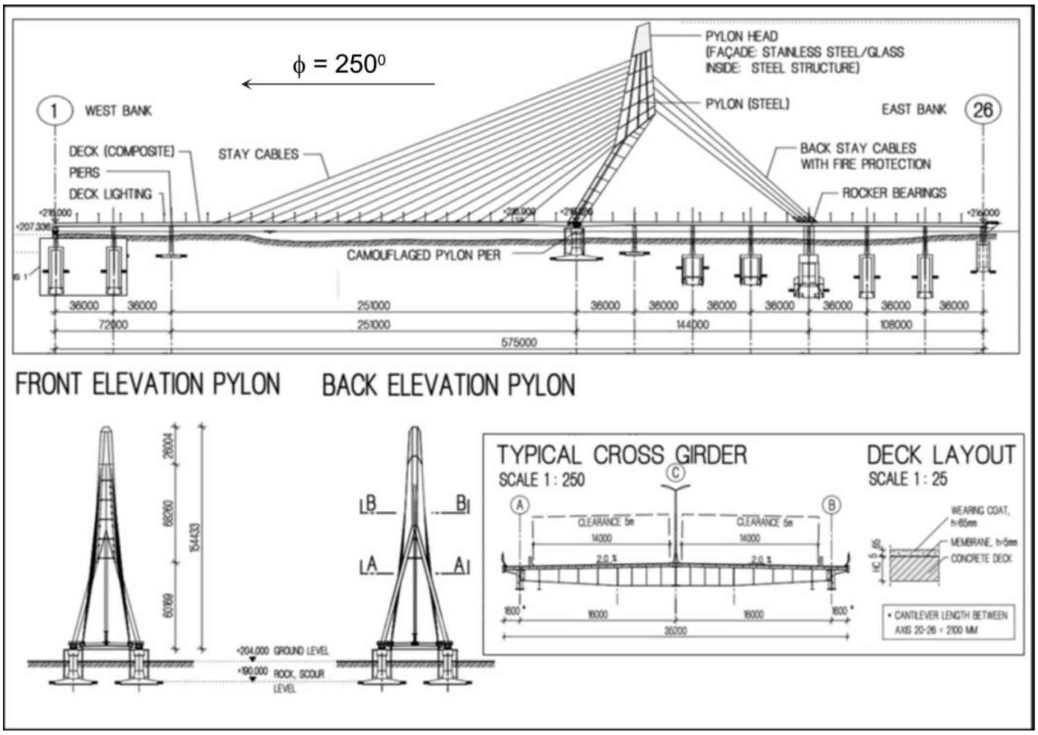

Fig. C1b NW-SE elevation and front and back views of pylon

Construction of the bridge began in 2010, and was completed in late 2018.

REFERENCES

1. Duvall, W.I. and Fogelson, D.E. (1962). "Review of Criteria for Estimating Damage to Residences from Blasting Vibrations", *U.S. Dept. of the Interior, Bureau of Mines, Report of Investigations*, R.I. No. 5968.
2. Gupta, I.D. (2007). "Probabilistic Seismic Hazard Analysis Method for Mapping of Various Parameters to Estimate the Earthquake Effects on Manmade Structures", *Indian Society of Earthquake Technology Journal,* Vol. 44, No. 1, pp. 127–167.
3. Gupta, I.D., Tripathy, G.R. and Shirke, R.R. (2003). "Controlled Blasting for Rock Excavation in Civil Engineering Applications", *Government of India ministry of water resources, Technical Memorandum, Central Water and Power Research Station*, Khadakwasla, Pune, India.
4. Gupta, I.D. and Trifunac, M.D. (2017). "Scaling of Fourier Spectra of Strong Earthquake Ground Motion in Western Himalaya and Northeastern India", *Soil Dynamics and Earthquake Engineering,* Vol. 106, pp. 137-159.
5. Gupta, I.D. and Trifunac, M.D. (2018a). "Empirical Scaling Relations for Pseudo Relative Velocity Spectra in Western Himalaya and Northeast India", *Soil Dynamics and Earthquake Engineering,* Vol. 106, pp. 70-89.
6. Gupta, I.D. and Trifunac, M.D. (2018b). "Attenuation of Strong Earthquake Ground Motion – II: Dependence on Geology Along the wave Paths from the Burmese Subduction Zone to Northeastern India", *Soil Dynamics and Earthquake Engineering*, Vol. 112, pp. 256-276.
7. Gupta, I.D. and Trifunac, M.D. (2018c). "Attenuation of Strong Earthquake Ground Motion – I: Dependence on Geology Along the Wave Paths from the Hindu Kush Subduction Zone to Western Himalaya", *Soil Dynamics and Earthquake Engineering*, Vol. 114, pp. 127-145.
8. Gupta, I.D. and Trifunac, M.D. (2019). "Attenuation of Fourier Amplitude and Pseudo Relative Velocity Spectra Due to Local Earthquakes in the National Capital Region of India", *Soil Dynamics and Earthquake Engineering*, Vol. 116, pp. 593-611.
9. Gupta, I.D., and Trifunac, M.D. (2023). "Attenuation of the Peaks of Earthquake Ground Motion Along the Himalayan Orogenic Belt", *ISET Journal of earthquake Technology*, Vol. 60, No. 3, pp.75–99
10. Gupta, I.D., Lee, V.W. and Trifunac, M.D. (2022a). "Seismic Microzonation of Delhi Metropolitan Area. India – I: Modeling of Seismicity", *Earthquake Engineering and Resilience*, Vol. 1, pp. 115-137.
11. Gupta, I.D., Lee, V.W. and Trifunac, M.D. (2022b). "Seismic Microzonation of Delhi Metropolitan Area. India – II: Hazard computation and Zoning Maps", *Earthquake Engineering and Resilience,* Vol. 1, pp. 138-163.
12. Gusev, A.A. (1983). "Descriptive Statistical Model of Earthquake Source Radiation and its Application to an Estimation of Short-Period Strong Motion", *Geophysical Journal of the Royal Astronomical Society,* Vol. 74, No. 3, pp. 787–808.
13. Langefors, U. and Kihlström, B. (1978). "Modern Technique for Rock Blasting", J. Wiley, New Jersey, U.S.
14. Lee, V.W. and Trifunac, M.D. (1985). "Uniform Risk Spectra of Strong Earthquake Ground Motion", *Department of Civil Engineering, Report CE 85-05,* University of Southern Calif., Los Angeles, California.
15. Lee, V.W. and Trifunac, M.D. (1987). "Microzonation of a Metropolitan Area", *Department of Civil Engineering, Report CE 87-02*, University of Southern California, Los Angeles, California.
16. Todorovska, M.I. and Trifunac, M.D. (1996a). "A Seismic Hazard Model for Peak Strains in Soils During Strong Earthquake Shaking", *Earthquake Engineering and Engineering Vibration,* Vol. 16, Supplement, pp. 1-12.
17. Todorovska, M.I. and Trifunac, M.D. (1996b). "Hazard Mapping of Normalized Peak Strain in Soil During Earthquakes - Microzonation of a Metropolitan Area", *Soil Dynamics and Earthquake Eng.*, Vol. 15, No. 5, pp. 321-329.

18. Todorovska, M.I. and Trifunac, M.D. (1998). "Discussion of The Role of Earthquake Hazard Maps in Loss Estimation: A Study of the Northridge Earthquake, by R.B. Olshansky, Earthquake Spectra", Vol. 14, No. 3, pp. 557-563.
19. Todorovska, M.I., Lee, V.W. and Trifunac, M.D. (2007). "Shaking Hazard Compatible Methodology for Probabilistic Assessment of Permanent Ground Displacement Across Earthquake Faults", *Soil Dynamics and Earthquake Engineering*, Vol. 27, No. 6, pp. 586–597.
20. Trifunac, M.D. (1992). "Should Peak Accelerations be used to Scale Design Spectrum Amplitudes?" *Proc. 10th World Conf. Earthquake Eng*., Madrid, Spain, Vol. 10, pp. 5817-5822.
21. Trifunac, M.D. (2012). "Earthquake Response Spectra for Performance based Design – A Critical Review", *Soil Dynamics and Earthquake Engineering*, Vol. 37, No. 6, pp. 73-83.
22. Trifunac, M.D. (2013). "Scaling Response Spectra by Peak Ground Acceleration Violates the Performance-Based Design Objectives", Izgradnja, No. 5-6, pp. 187-286.
23. Trifunac, M.D. (2016). "Site Conditions and Earthquake Ground Motion – A Review", *Soil Dynamics and Earthquake Engineering*, Vol. 90, pp. 88-100.
24. Trifunac, M.D. and A.G. Brady (1975). "On the Correlation of Seismic Intensity Scales with the Peaks of Recording Strong Ground Motion", *Bulletin of the Seismological Society of America*, Vol. 65, No. 1, pp. 139-162.
25. Trifunac, M.D. and Gičev, V. (2006). "Response Spectra for Differential Motion of Columns, Paper II: Out-of-Plane Response", *Soil Dynamics and Earthquake Engineering*, Vol. 26, No 12, pp. 1149-1160.
26. Trifunac, M.D. and Lee, V.W. (1996). "Peak Surface Strains During Strong Earthquake Motion", *Soil Dynamics and Earthquake Eng*., Vol. 15, No. 5, pp. 311-319.
27. Trifunac, M.D. and Todorovska, M.I. (1997). "Response Spectra and Differential Motion of Columns", *Earthquake Eng. and Structural Dyn.*, Vol. 26, No. 2, pp. 251-268.